

# A new genus and species of Cryphonectriaceae causing stem cankers on plantation eucalypts in South Africa

Hiroyuki Suzuki<sup>1,2</sup>  | Seonju Marincowitz<sup>1</sup> | Jolanda Roux<sup>3,4</sup> | Trudy Paap<sup>1</sup> | Brenda D. Wingfield<sup>1</sup> | Michael J. Wingfield<sup>1</sup>

<sup>1</sup>Department of Biochemistry, Genetics and Microbiology, Forestry and Agricultural Biotechnology Institute (FABI), University of Pretoria, Hatfield, South Africa

<sup>2</sup>Faculty of Agro-Food Science, Niigata Agro-Food University, Tainai, Japan

<sup>3</sup>Department of Plant and Soil Sciences, Forestry and Agricultural Biotechnology Institute (FABI), University of Pretoria, Hatfield, South Africa

<sup>4</sup>Sappi Ltd, Sappi Shaw Research Centre, Howick, South Africa

## Correspondence

Hiroyuki Suzuki, Department of Biochemistry, Genetics and Microbiology, Forestry and Agricultural Biotechnology Institute (FABI), University of Pretoria, Private Bag X20, Hatfield, 0002, South Africa.  
Email: [hiroyuki-suzuki@nafu.ac.jp](mailto:hiroyuki-suzuki@nafu.ac.jp)

## Funding information

University of Pretoria; the Tree Protection Co-operative Programme (TPCP) South Africa

## Abstract

Fungi in the Cryphonectriaceae are important canker pathogens of woody shrubs and trees in the Melastomataceae and Myrtaceae (Myrtales). During 2021 disease surveys in KwaZulu-Natal (South Africa) plantations, a serious stem canker disease was discovered on species of *Eucalyptus* and *Corymbia*. The cankers had structures on their surfaces typical of fungi in the Cryphonectriaceae. The aims of the study were to identify the fungus associated with the disease and to test its pathogenicity. Morphological characteristics of both sexual and asexual structures and phylogenetic analyses based on partial sequences of the conserved nuclear large subunit (LSU) ribosomal DNA, the internal transcribed spacer (ITS) regions including the 5.8S gene of the ribosomal DNA operon, and two  $\beta$ -tubulin (*BT1/BT2*) regions were used for identification purposes. Phylogenetic analyses of the sequence data and morphological characteristics supported the establishment of a new genus in the Cryphonectriaceae, for which the name *Xanthoportha myrticola* gen. et sp. nov. is provided. Pathogenicity trials showed that isolates were pathogenic on tested *Eucalyptus grandis* and hybrids as well as *Corymbia henryi*. The results suggest that this is an emerging pathogen that could influence the sustainability of plantation forestry in South Africa.

## KEYWORDS

*Corymbia*, *Eucalyptus*, taxonomy, Cryphonectriaceae

## 1 | INTRODUCTION

The Cryphonectriaceae accommodates some of the world's most important tree pathogens. The best known of these is *Cryphonectria parasitica*, the causal agent of chestnut blight, which destroyed native stands of American chestnut (*Castanea dentata*) and European chestnut (*Castanea sativa*) in their natural habitats (Anagnostakis & Kranz, 1987). The Cryphonectriaceae accommodates approximately 30 genera, including many species that are pathogens causing blight, die back or canker on stems of trees (Gryzenhout et al., 2009; Jiang et al., 2020; Rauf et al., 2019). An emerging group of these fungi, occurring mostly in the tropics and southern hemisphere, occur on woody shrubs and trees in the Myrtales, especially

the Melastomataceae and Myrtaceae (Ali et al., 2018; Begoude et al., 2010; Beier et al., 2015; Chen et al., 2016, 2018; Crane & Burgess, 2013; Ferreira et al., 2019; Gryzenhout et al., 2009; Huang et al., 2022; Vermeulen et al., 2011). Of these fungi, species in the genus *Chrysoportha*, first described to accommodate the *Eucalyptus* pathogen *Cryphonectria cubensis*, are best known (Gryzenhout et al., 2004, 2009).

Ten species residing in six genera of the Cryphonectriaceae are known to occur in South Africa. Other than *Immersiportha knoxdaviesiana*, which causes a serious canker disease on *Rapanea melanophloes* (Myrsinaceae) (Chen, Wingfield, Roets, & Roux, 2013), these are all pathogens of trees in the Myrtaceae (Ali et al., 2018; Chen, Wingfield, & Roux, 2013; Gryzenhout et al., 2004; Nakabonge,

Gryzenhout, et al., 2006; Vermeulen et al., 2011, 2013). From a commercial forestry perspective, the most important of these pathogens in South Africa is *Chrysosporthe austroafricana*, which causes a serious canker disease on *Eucalyptus* spp. (Gryzenhout et al., 2004; Nakabonge, Roux, et al., 2006; Vermeulen et al., 2013), and *Corymbia henryi* (Suzuki et al., 2023).

*C. austroafricana* (as *Cryphonectria cubensis*) was first discovered in South Africa, causing cankers on *Eucalyptus* in 1988 (Wingfield et al., 1989). Subsequently, many studies have been conducted on the fungus and the disease that it causes. Early taxonomic studies showed that it resided in a genus distant from *Cryphonectria*, leading to the establishment of the new genus *Chrysosporthe* to accommodate it (Gryzenhout et al., 2004). The pathogen was shown to be native to Southern Africa, having undergone a host shift (Slippers et al., 2005) from native Myrtaceae (Nakabonge, Roux, et al., 2006; Vermeulen et al., 2013). Although the disease occasionally appears in plantations, it has been effectively managed through tree breeding and the selection of disease-tolerant *Eucalyptus* hybrid clones (Van Heerden et al., 2005; Wingfield, 2003; Wingfield et al., 2013).

Recent disease surveys in KwaZulu-Natal plantations revealed cankers on *Eucalyptus grandis*, *Eucalyptus urophylla* × *E. grandis* hybrid trees and *C. henryi* bearing fruiting bodies of a fungus in the Cryphonectriaceae (Figure 1). The gross morphology of the fungal structures on these cankers was atypical of those caused by *C.*

*austroafricana*. The aims of this study were to identify the fungus associated with the canker disease and to test its pathogenicity on *E. grandis* varieties and *C. henryi*, thus evaluating its relevance to plantation forestry in South Africa.

## 2 | MATERIALS AND METHODS

### 2.1 | Sampling and isolations

Fruiting structures similar to those typical of the Cryphonectriaceae were found on the bark, covering cankers on *C. henryi* (4 years old) close to the town of KwaNgwanase, KwaZulu-Natal Province of South Africa in mid-2020. Subsequently, similar fruiting structures were found on the stems of *E. grandis* (1 year old) and *E. urophylla* × *E. grandis* (1 year old) hybrid varieties in Mtubatuba, KwaZulu-Natal in mid-2021 and 2022, and from *E. grandis* and *E. urophylla* × *E. grandis* hybrid varieties near the city of Richards Bay in 2022 (Figure 1, Figure S1).

Bark samples bearing fungal fruiting bodies were collected from the stems of infected *C. henryi*, *E. grandis* and *E. urophylla* × *E. grandis*. These were placed individually in brown paper bags and transported to the laboratories of the Forestry and Agricultural Biotechnology Institute (FABI), University of Pretoria for further study. One fruiting structure from each of 12 *C. henryi* bark samples, eight *E. grandis*



**FIGURE 1** Symptoms associated with infection of young trees (1 year old) of a *Eucalyptus urophylla* × *E. grandis* hybrid variety. (a) Trees dying in a plantation. (b–d) Cracking bark and discolouration of the stems at the root collar region with distinct infection of the cambial tissues (arrow).

bark samples, and two *E. urophylla* × *E. grandis* bark samples were used for isolation. Fruiting structures were dissected with a sterile scalpel under a dissection microscope. The exposed spores and inner structures of the fruiting bodies were spread over the surface of 2% malt extract agar (MEA: 20g BioLab malt extract, 20g Difco Bacto agar, 1L deionized water, supplemented with 100mg/L streptomycin) in Petri dishes. A small block of MEA containing a single hyphal tip was transferred with a sterilized needle to fresh MEA, and pure cultures were allowed to grow at 23°C in the dark. The cultures were deposited in the culture collection (CMW) of FABI, University of Pretoria, Pretoria, South Africa. Isolates representing ex-holotype and ex-paratypes of the novel genus are maintained in the culture collection of Innovation Africa (CMW-IA), University of Pretoria. Dried type specimens have been deposited in the H.G.W.J. Schweickerdt Herbarium (PRU), University of Pretoria, South Africa.

## 2.2 | Phylogenetic analysis

Total genomic DNA was extracted from 7-day-old cultures growing on MEA using PrepMan Ultra Sample preparation reagent (Applied Biosystem) following the manufacturer's protocols. PCRs were performed to amplify the internal transcribed spacer (ITS) regions, including the 5.8S gene of the ribosomal RNA, 28S large subunit (LSU), and partial sequences of the  $\beta$ -tubulin (*BT1*, *BT2*) gene region. The primer pairs ITS1/ITS4 (White et al., 1990), LR0R/LR7 (Rehner & Samuels, 1994; Vilgalys & Hester, 1990), and BT1a/BT1b and BT2a/BT2b (Glass & Donaldson, 1995) were used for amplification of the ITS, LSU and *BT* regions, respectively. The PCRs were conducted as described by Suzuki et al. (2023). After the PCR products were purified using ExoSAP-IT (Affymetrix), the amplicons stained with GelRed (Biotium) were visualized using gel electrophoresis.

A sequencing reaction was conducted with either the forward or reverse primer using the ABI PRISM BigDye Terminator Cycle Sequencing Ready Reaction kit v. 3.1 (Applied BioSystems). An ABI PRISM 3100 Autosequencer (Applied BioSystems) was used to generate the sequences. The raw sequences were assembled using MEGA7 (Kumar et al., 2016).

The sequences of 44 isolates representing genera of Cryphonectriaceae closely related to the fungus under investigation were obtained from GenBank (<http://www.ncbi.nlm.nih.gov>) and combined into datasets for analyses with isolates obtained in this study (Table 1). Each sequenced region was analysed separately. Because sequences for the LSU region of some of the isolates were not available, the sequences of ITS and *BT* regions were combined and analysed. The datasets were aligned using MAFFT v. 7 with the G-INS-I option (Katoh et al., 2019). The substitution model was selected for each region and combined datasets with the Akaike information criterion (AIC) in jModelTest v. 2.1.5 (Posada, 2008). Maximum-likelihood (ML) analysis was conducted using PhyML with 1000 replicate bootstrap analyses (Guindon et al., 2010). Bayesian inference analyses were performed using MrBayes v. 3.2.1 (Ronquist et al., 2012) to estimate the posterior probabilities

of the tree topologies with Metropolis-coupled Markov chain Monte Carlo searches. The analysis was conducted for 3,000,000 generations with four runs. Trees were sampled every 100 generations, and a 25% burn-in was used to summarize a consensus tree. *Amphylogia gyrosa* and *Chrysomorbus lagerstroemiae*, belonging to the Cryphonectriaceae, were chosen as the outgroup taxa.

## 2.3 | Morphological observations

Fungal structures were initially mounted in water that was replaced with 85% lactic acid. Measurements were made, and images were captured using Nikon Eclipse Ni and SMZ18 microscopes mounted with a DS-Ri2 camera. Bark tissues containing fruiting structures were boiled for a few seconds to soften the woody structures. The tissues were cut into small pieces (approx. 5 × 5 mm) and mounted in a tissue-freezing medium (Leica). Vertical sections between 10 and 12  $\mu$ m thick were cut from the selected tissue samples to observe the configuration of fruiting structures in the bark. The measurements were presented as minimum–maximum (average  $\pm$  SD, *n* = the number of measurements).

Culture growth characteristics were studied in 90mm Petri dishes containing 2% MEA. To assess growth in culture, 6-day-old mycelial plugs (5mm diameter) were placed at the centres of the Petri dishes. These were incubated at temperatures between 5 and 35°C at 5-degree intervals in the dark. Five replicate plates were prepared for each temperature. Mycelial growth was checked daily until the colonies reached the edges of the plates at the optimal temperature for growth, at which time the experiment was terminated. Two diameter measurements were taken perpendicular to each other for each culture, and the averages were determined. These averages were used to calculate a daily growth rate. Culture characteristics were noted first when the colonies reached the edge of the plate at the optimum growth temperature, and a second observation was made when these cultures were 30 days old.

## 2.4 | Pathogenicity tests

Two isolates (CMW 56597 and CMW 57827) were used to test pathogenicity on 1-year-old *E. grandis* varieties (GC540, TAG5 and ZG14) and *C. henryi* saplings grown in potting bags. The stem diameters of the saplings were between 9 and 16 mm. Ten of each *Eucalyptus* variety and 20 *C. henryi* saplings were inoculated with discs taken from the actively growing edges of 14-day-old cultures of each of the two isolates. An equal number of each of the *E. grandis* varieties and 14 *C. henryi* saplings were treated with discs of water agar (WA; 20g Difco Bacto agar, 1L deionized water) to serve as negative controls.

For inoculation, a disc of bark was removed from the stems of the plants about 30 cm above ground level using a cork borer (5 mm diameter) to expose the cambium. Agar discs containing mycelium of the fungus or sterile agar were placed into the wounds and covered with Parafilm (Bemis) to reduce desiccation and contamination

TABLE 1 Isolates and sequences used for phylogenetic analysis.

Species	Isolate <sup>a</sup>	Location	Host	GenBank accession number <sup>b</sup>			LSU
				ITS	BT1	BT2	
<i>Aurapex penicillata</i>	CMW10030 <sup>c</sup>	Colombia	<i>Miconia theaezans</i>	AY214311	AY214239	AY214275	AY194103
	CMW11295	Colombia	<i>M. theaezans</i>	AY214314	AY214242	AY214278	AY194089
<i>Corticimorbus sinomyrti</i>	CERC3634	China	<i>Rhodomyrtus tomentosa</i>	KT167171	KT167191	KT167191	KT167181
	CMW44650 <sup>c</sup>	China	<i>R. tomentosa</i>	KT167169	KT167189	KT167189	NG060424
<i>Cryphonectria decipiens</i>	CMW10484	Italy	<i>Castanea sativa</i>	AF368327	AH011606	AH011606	—
	CMW10436	Portugal	<i>Quercus suber</i>	AF452117	AF525703	AF525710	JQ862750
<i>Cryphonectria japonica</i>	CMW10527 <sup>c</sup>	Russia	—	DQ120761	DQ120767	DQ120768	—
	CMW10528	Russia	—	DQ120760	DQ120765	DQ120766	AF408340
<i>Cryphonectria macrospora</i>	CMW10463	Japan	—	AF368331	AF368351	AF368350	—
	CMW10914	Japan	—	AY697942	AY697973	AY697974	—
<i>Cryphonectria naterciae</i>	CO614	Portugal	<i>Q. suber</i>	EU442651	EU442660	EU442660	—
	CO679	Portugal	<i>Q. suber</i>	EU442652	EU442661	EU442661	—
<i>Cryphonectria nitschkei</i>	CMW10518 <sup>c</sup>	Japan	<i>Quercus grosseserrata</i>	AF452118	AF525706	AF525713	—
	CMW13742	Japan	<i>Q. grosseserrata</i>	AY697936	AY697961	AY697962	—
<i>Cryphonectria parasitica</i>	CMW7048	USA	<i>Quercus virginiana</i>	AF368330	AF273076	AF273470	AY194100
<i>Cryphonectria quercicola</i>	CMW14547	Azores	<i>C. sativa</i>	DQ368749	DQ368751	DQ368752	—
	CFCC52140	China	<i>Quercus wutaishansea</i>	MG866026	MG896117	MG896113	—
<i>Cryphonectria quercus</i>	CFCC52141	China	<i>Q. wutaishansea</i>	MG866027	MG896118	MG896114	—
	CFCC52138	China	<i>Quercus aliena</i> var. <i>acuteserrata</i>	MG866024	MG896111	MG896115	—
<i>Cryphonectria radicalis</i>	CFCC52139	China	<i>Q. aliena</i> var. <i>acuteserrata</i>	MG866025	MG896112	MG896116	—
	CMW10455	Italy	<i>Q. suber</i>	AF452113	AF525705	AF525712	AY194101
<i>Cryptometrion aestuescens</i>	CMW10477	Italy	<i>Q. suber</i>	AF368328	AH011607	AH011607	AY194102
	CMW18790	Indonesia	<i>Eucalyptus grandis</i>	GQ369458	GQ369455	GQ369455	HQ171211
<i>Diversimorbus metrosiderotis</i>	CMW28535 <sup>c</sup>	Indonesia	<i>E. grandis</i>	GQ369457	GQ369454	GQ369454	HQ171212
	CMW37321	South Africa	<i>Metrosideros angustifolia</i>	JQ862870	JQ862911	JQ862952	JQ862827
<i>Holocryphia capensis</i>	CMW37322 <sup>c</sup>	South Africa	<i>M. angustifolia</i>	JQ862871	JQ862912	JQ862953	JQ862828
	CMW37331	South Africa	<i>M. angustifolia</i>	JQ862860	JQ862901	JQ862942	JQ862817
<i>Holocryphia eucalypti</i>	CMW37887 <sup>c</sup>	South Africa	<i>M. angustifolia</i>	JQ862854	JQ862895	JQ862936	JQ862811
	CMW7033	South Africa	<i>E. grandis</i>	JQ862837	JQ862878	JQ862919	JQ862794
<i>Holocryphia glienana</i>	CMW7036 <sup>c</sup>	South Africa	<i>Eucalyptus</i> sp.	AF232878	AF368341	AF368340	JQ862796
	CMW37334 <sup>f</sup>	South Africa	<i>M. angustifolia</i>	JQ862834	JQ862875	JQ862916	JQ862791
<i>Holocryphia mzansi</i>	CMW37335	South Africa	<i>M. angustifolia</i>	JQ862835	JQ862876	JQ862917	JQ862792
	CMW37337 <sup>f</sup>	South Africa	<i>M. angustifolia</i>	JQ862841	JQ862882	JQ862923	JQ862798
	CMW37338	South Africa	<i>M. angustifolia</i>	JQ862842	JQ862883	JQ862924	JQ862799



TABLE 1 (Continued)

Species	GenBank accession number <sup>b</sup>						
	Isolate <sup>a</sup>	Location	Host	ITS	BT1	BT2	LSU
<i>Luteocirithus shearii</i>	CBS130775	Australia	<i>Banksia baxteri</i>	KC197024	KC197015	KC197009	KC197018
	CBS130776 <sup>c</sup>	Australia	<i>B. baxteri</i>	KC197021	KC197012	KC197006	KC197019
<i>Parvomorbus eucalypti</i>	CSF2061 <sup>c</sup>	China	<i>E. urophylla</i> × <i>E. grandis</i>	MN258788	MN258816	MN258802	MN258844
	CSF2062	China	<i>E. urophylla</i> × <i>E. grandis</i>	MN258789	MN258817	MN258803	MN258845
<i>Parvomorbus guangdongensis</i>	CSF10438	China	<i>E. urophylla</i> hybrid clone	MN258796	MN258824	MN258810	MN258852
	CSF10460 <sup>c</sup>	China	<i>E. urophylla</i> hybrid clone	MN258799	MN258827	MN258813	MN258855
<i>Xanthoportha myrticola</i>	CMW56597	South Africa	<i>Corymbia henryi</i>	PP058388	PP061188	PP061188	PP058407
	CMW56598	South Africa	<i>C. henryi</i>	PP058389	PP061189	PP061189	PP058408
	CMW56604	South Africa	<i>C. henryi</i>	PP058390	PP061190	PP061190	PP058409
	CMW56605	South Africa	<i>C. henryi</i>	PP058391	PP061191	PP061191	PP058410
	CMW56611	South Africa	<i>C. henryi</i>	PP058392	PP061192	PP061192	PP058411
	CMW56612	South Africa	<i>C. henryi</i>	PP058393	PP061193	PP061193	PP058412
	CMW56619	South Africa	<i>C. henryi</i>	PP058394	PP061194	PP061194	PP058413
	CMW57819	South Africa	<i>E. grandis</i>	PP058395	PP061195	PP061195	PP058414
	CMW57820	South Africa	<i>E. grandis</i>	PP058396	PP061196	PP061196	PP058415
	CMW57822	South Africa	<i>E. grandis</i>	PP058397	PP061197	PP061197	PP058416
	CMW57823	South Africa	<i>E. grandis</i>	PP058398	PP061198	PP061198	PP058417
	CMW57824	South Africa	<i>E. grandis</i>	PP058399	PP061199	PP061199	PP058418
	CMW57825	South Africa	<i>E. grandis</i>	PP058400	PP061200	PP061200	PP058419
	CMW57826	South Africa	<i>E. grandis</i>	PP058401	PP061201	PP061201	PP058420
	CMW57827	South Africa	<i>E. urophylla</i> × <i>E. grandis</i>	PP058402	PP061202	PP061202	PP058421
	CMW57829	South Africa	<i>C. henryi</i>	PP058403	PP061203	PP061203	PP058422
CMW57830	South Africa	<i>C. henryi</i>	PP058404	PP061204	PP061204	PP058423	
CMW57831	South Africa	<i>C. henryi</i>	PP058405	PP061205	PP061205	PP058424	
CMW58507 <sup>c</sup>	South Africa	<i>E. urophylla</i> × <i>E. grandis</i>	PP058406	PP061206	PP061206	PP058425	
<i>Amphilogia gyrosa</i>	CMW10469 <sup>c</sup>	New Zealand	<i>Elaeocarpus dentatus</i>	AF452111	AF525707	AF525714	AY194107
	CMW10470	New Zealand	<i>E. dentatus</i>	AF452112	AF525708	AF525715	AY194108
<i>Chrysomorbus lagerstroemiae</i>	CERC8810 <sup>c</sup>	China	<i>Lagerstroemia speciosa</i>	KY929338	KY929358	KY929358	KY929328
	CERC8812	China	<i>L. speciosa</i>	KY929339	KY929359	KY929349	KY929329

Note: Isolates presented in bold were sequenced in this study.

<sup>a</sup>CMW, the culture collection of the Forestry & Agricultural Biotechnology Institution (FABI), University of Pretoria, Pretoria; CERC, China Eucalypt Research Centre, Zhanjiang, Guangdong, China; CFCC, China Forestry Culture Collection Center, Beijing, China; CBS, Centraalbureau voor Schimmelcultures, Utrecht, Netherlands; CSF, Culture Collection from Southern Forests, Zhanjiang, Guangdong, China.

<sup>b</sup>ITS, internal transcribed spacers and intervening 5.8S rDNA; BT1 and BT2, partial  $\beta$ -tubulin gene; LSU, 28S rRNA large subunit.

<sup>c</sup>Ex-type.

(Continues)

of the inoculum. Lesion development was evaluated after 6 weeks by measuring the bark lesions as well as by scraping away the bark to expose the cambium allowing for lesion lengths to be measured. Small pieces of bark and cambium were removed from the edges of the lesions and transferred to 2% MEA plates for reisolation of the inoculated fungus. Where fruiting bodies were visible on the diseased bark, isolations were also made directly from them.

Statistical analyses at a 5% significance level on the lesion length data were performed using R (R Core Team, 2019). The data from the *Eucalyptus* varieties and *C. henryi* saplings were analysed separately because inoculation experiments on the *Eucalyptus* varieties and *C. henryi* saplings were conducted separately. A Grubbs test was used to detect outliers of the length with the 'outliers' package (Shiffler, 1988). Normality and homogeneity of variance of the data were tested using the Shapiro–Wilk test and Bartlett test. The data from the inoculation test on the *Eucalyptus* varieties were then subjected to one-way analysis of variance (ANOVA) followed by a Games–Howell post hoc test, while the data from the inoculations on *C. henryi* were subjected to the Kruskal–Wallis test followed by the Steel–Dwass test with 'PMCMRplus' package (Pohlert, 2020).

### 3 | RESULTS

#### 3.1 | Sampling and isolation

Fungal fruiting bodies were visible on the cracked bark on the root collar cankers of dying trees. In some instances, yellow drops of spores, typical of the Cryphonectriaceae, were seen exuding from these fruiting bodies. Black necks were visible for some fruiting bodies, while others were characterized by light yellow to orange stromatic structures immersed in the bark. Nineteen pure cultures having an appearance typical of species in the Cryphonectriaceae were obtained from infected trees. All of the isolates were used in the phylogenetic analysis, and four of these were subjected to morphological analyses.

#### 3.2 | DNA sequencing and phylogenetic analysis

All sequences obtained for the 19 isolates collected in this study were deposited in GenBank (Table 1). The aligned sequences for the ITS (615 bp), *BT* (959 bp) and LSU (491 bp) regions and combined sequences of ITS and *BT* datasets were deposited in Figshare (doi: 10.6084/m9.figshare.24920829). The dataset of the LSU region consisted of 50 taxa, and the rest included 63 taxa.

The 19 isolates resided in a clade closest to that accommodating the genus *Parvomorbus* (the corrected orthography of the original name, *Parvosmorbus* [MB 832455]), in all phylogenetic trees, regardless of the hosts from which they were isolated (Figure 2, Figure S2). The *Parvomorbus* clade was distinct from the clade accommodating isolates considered in the present study with a high support value (a bootstrap value of 88%–98% and BI of 1.0).

#### 3.3 | Taxonomy

*Xanthoportha* H. Suzuki, Jol. Roux, M.J. Wingf. & Marinc. gen. nov. Figures 3 and 4.

Mycobank MB 851635.

*Type:* *Xanthoportha myrticola* H. Suzuki, Jol. Roux, M.J. Wingf. & Marinc.

*Etymology:* Name 'Xantho' refers to the yellow/orange stromatic structures and 'porthē' (killer) the ability of the fungus to kill trees.

*Description:* **Ascostromata** semi-immersed, erumpent, pulvinate, consisting of valsoid perithecia. **Perithecia** single or grouped; *bases* immersed in the bark; *necks* emerge at stromatal surface as black ostioles covered with yellow stromatal tissue, papillate or short, above stromatal surface. **Asci** hyaline, broadly fusiform. **Ascospores** hyaline, fusoid to oval, with round ends, aseptate, straight, occasionally slightly curved. **Conidiomata** stromatic, immersed, erumpent, scattered, predominantly solitary, conical to subglobose; *locules* mostly uniloculate, occasionally multiloculate, convoluted; *necks* short, stout, mostly single, black, with yellow spore mass or tendril at tip. **Stromatic tissues** occasionally intermingled with host tissue, at base and side pseudoparenchymatous, *textura angularis*, around neck pseudoparenchymatous, *textura globulosa*. **Conidiophores** hyaline, branched at base, along the length immediately below transverse septa, smooth, septate, cylindrical, straight or irregular. **Paraphyses** present but scarce. **Conidiogenous cells** hyaline, phialidic, integrated, determinate, forming conidia from apical or lateral apertures immediately below transverse septa, subulate, lageniform to cylindrical. **Conidia** hyaline, cylindrical, aseptate, pointed towards base.

*Xanthoportha myrticola* H. Suzuki, Jol. Roux, M.J. Wingf. & Marinc. sp. nov. Figures 3 and 4.

Mycobank MB 851636.

*Etymology:* Name refers to the hosts of the fungus that resides in the Myrtaceae.

*Diagnosis:* Phylogenetically close to *Parvomorbus* spp. but differing from species in that genus by having fusoid to oval, aseptate ascospores and cylindrical conidia.

*Typus:* South Africa, KwaZulu-Natal Province, Mtubatuba, Plantation Trust, compartment E19, Bark of *Eucalyptus urophylla* × *grandis*. 31 March 2022. J. Roux. (Holotype PRU(M) 4504; exholotype culture CMW 58507, CMW-IA 163). GenBank: PP058406 (ITS); PP061206 ( $\beta$ -tubulin); PP058425 (LSU).

*Description:* **Ascostromata** on host substrate, gregarious, semi-immersed, erumpent, pulvinate, consisting of valsoid perithecia, occasionally intermingled with host tissue, edges pseudoparenchymatous, inner part prosenchymatous, tissues yellow to umber, covering the tops of perithecial base. **Perithecia** single or grouped; *bases* immersed in the bark; *necks* emerge at stromatal surface as black ostioles covered with yellow stromatal tissue, papillate or short, extending up to 469  $\mu$ m long ( $197 \pm 88.5 \mu$ m,  $n=25$ ) above stromatal surface, periphysate; *walls* pseudoparenchymatous, composed of layers of 6–12 horizontally flattened cells, outer layers consisting of pale brown to brown, thick-walled cells, inner layers consisting of hyaline, thin-walled cells, walls around necks consisting of brown,

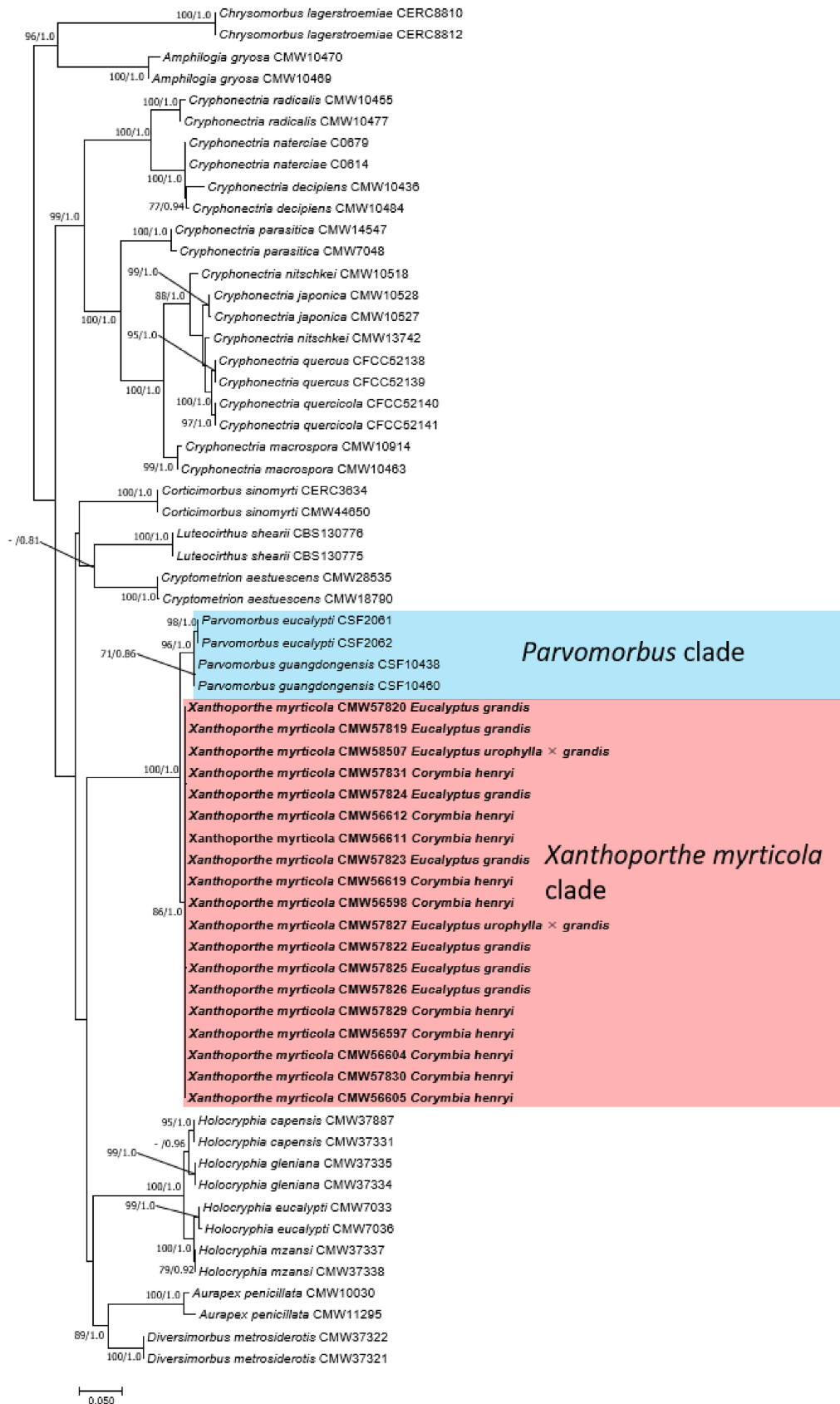
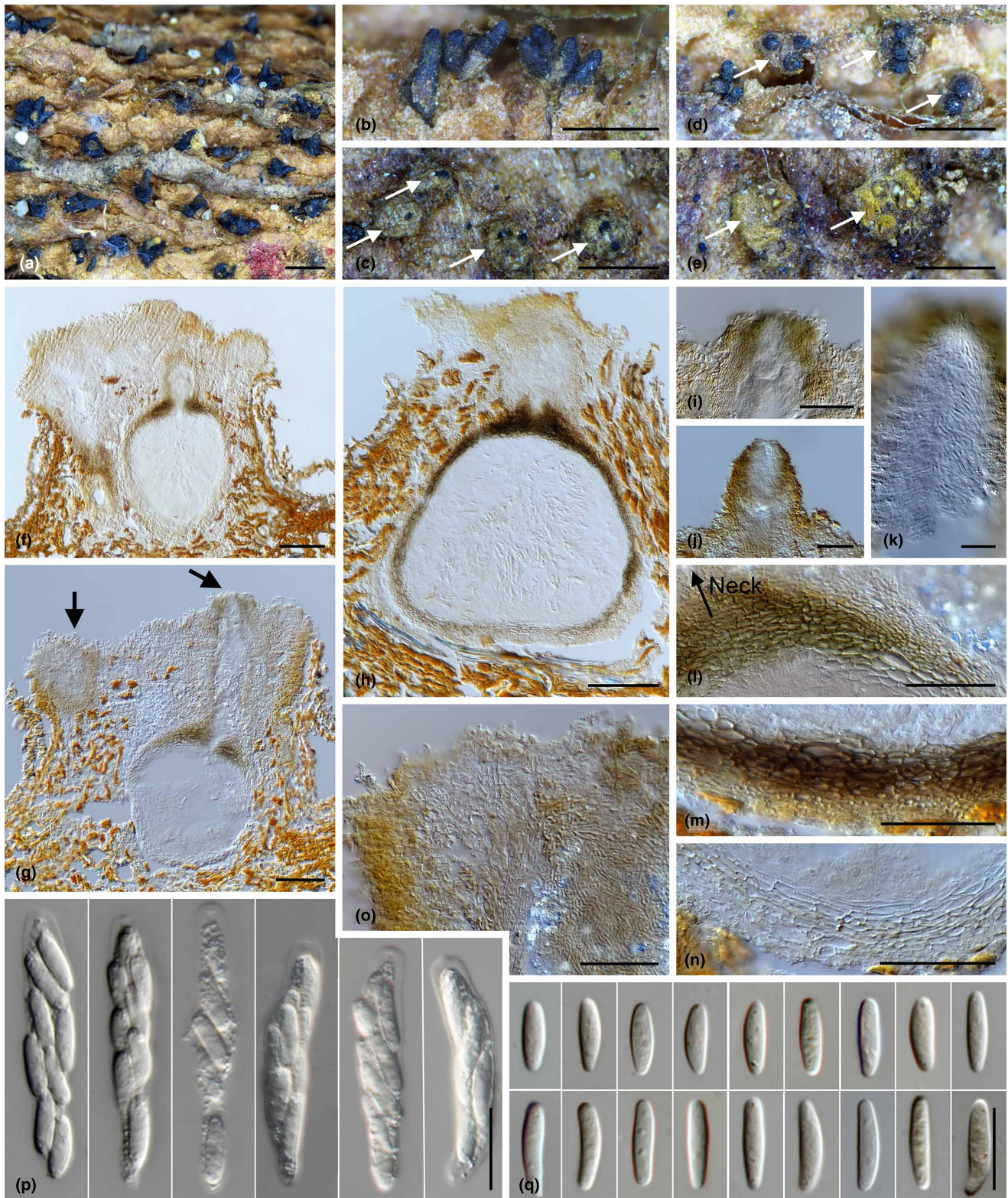
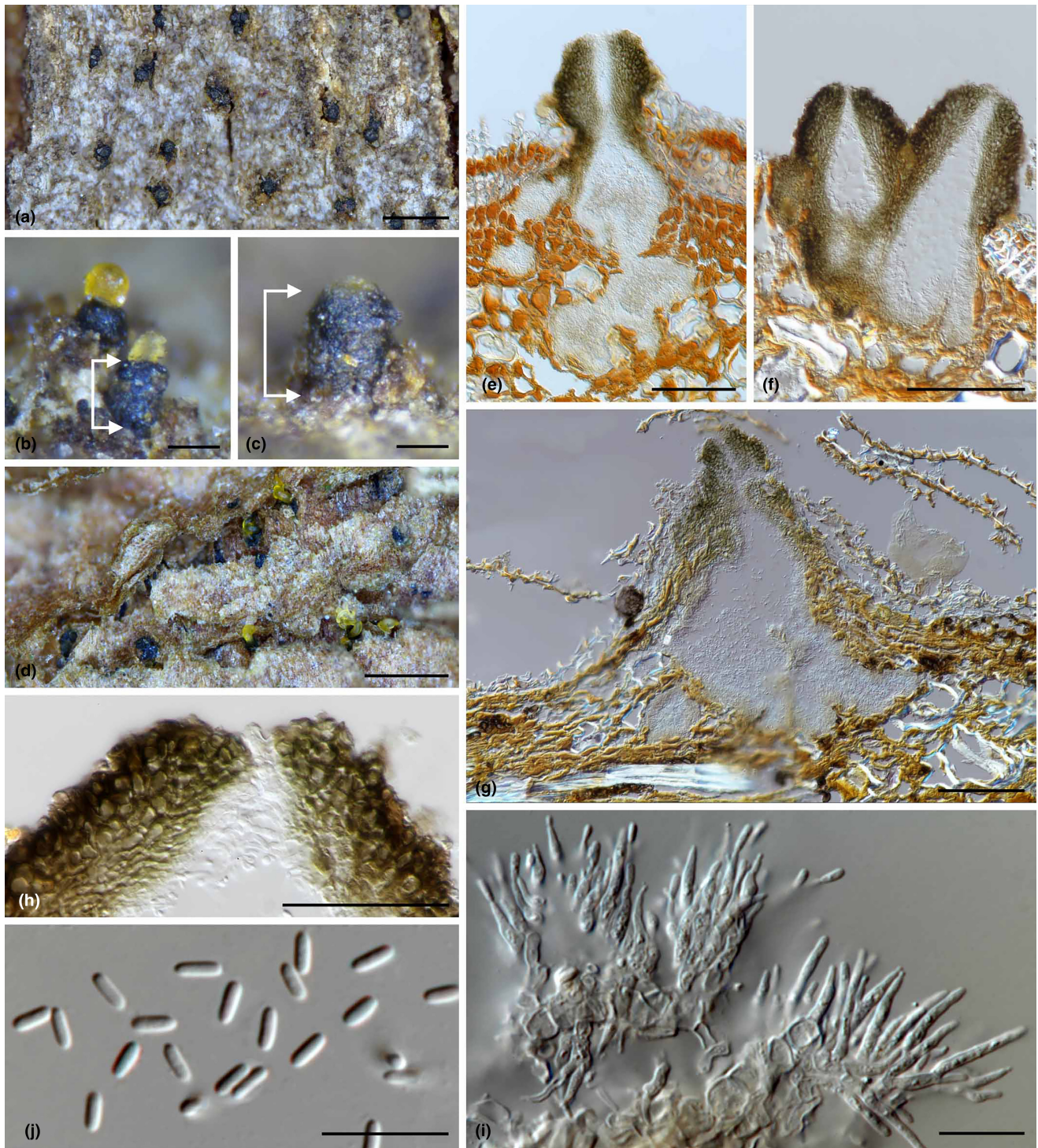


FIGURE 2 Phylogenetic tree based on maximum-likelihood (ML) analysis of a sequence dataset of combined region (ITS+BT) of the Cryphonectriaceae. The isolates in bold are those obtained during the current study. The bootstrap values >65% for ML and >0.8 for Bayesian inference posterior probabilities (BI PP) are shown as ML/BI PP. The *Parvomorbus* and *Xanthoportha myrticola* clades are highlighted in blue and red, respectively.



**FIGURE 3** Micrographs of sexual state of *Xanthoportha myrtilcola* sp. nov. (holotype, PRU(M) 4504; ex-holotype, CMW 58507, CMW-IA 163). (a–e) Ascostromata on the substrate, showing ascomatal necks emerged beyond the stromatal surface (b) and erumpent ascostromata (arrows) with single or multiple black necks (c–e; e, transversely truncated). (f–n) Vertical sections of ascostromata showing stromatic tissue covering the top of the perithecium (f); ascostromata having two necks (g, arrows); perithecial base (h); perithecial neck above the stromatal tissue (i, j); periphysate perithecial neck (k); and perithecial walls (l–n). (o) Stromatal structure where neck is developed. (p) Ascii. (q) Ascospores. Scale bars. a = 1000  $\mu\text{m}$ ; b–e = 500  $\mu\text{m}$ ; f–h, k = 100  $\mu\text{m}$ ; i, j, l–o = 50  $\mu\text{m}$ ; p, q = 10  $\mu\text{m}$ .



**FIGURE 4** Micrographs of asexual state of *Xanthoportha myrtilcola* sp. nov. on *Eucalytus urophylla* × *E. grandis* (PRU(M) 4504, CMW 58507, CMW-IA 163) (d, g, j) and on *Corymbia henryi* (PRU(M) 4506, CMW 56597, CMW-IA 165) (a–c, e, f, h, i). (a–d) Conidiomata in the substrate (arrows show the length of necks). (e–g). Vertical sections of conidioma showing convoluted locule and protruding neck. (h)Periphysate ostiole. (i) Conidiophores. (j) Conidia. Scale bars: a, d = 500  $\mu$ m; b, c, e–g = 100  $\mu$ m; h = 50  $\mu$ m; i, j = 10  $\mu$ m.

thick-walled cells. **Asci** hyaline, broadly fusiform, octosporous, 30–48 × 5–8 (35.7 ± 4.91 × 6.7 ± 0.86  $\mu$ m,  $n$  = 25). **Ascospores** hyaline, fusoid to oval, with round ends, aseptate, straight, occasionally slightly curved, 7–12 × 2–3.5 (9.7 ± 1.04 × 2.6 ± 0.29  $\mu$ m,  $n$  = 50).

**Conidiomata** on host substrate, stromatic, immersed, erumpent, scattered, predominantly solitary, conical to subglobose, fuscous black, 144–425 × 109–375 (285.1 ± 71.18 × 238.9 ± 72.88  $\mu$ m,  $n$  = 38); **locules** mostly uniloculate, occasionally multiloculate,

convoluted; necks short, stout (not attenuating), periphysate, mostly single, black, with yellow spore mass or tendril at tip; walls pale brown to dark brown. **Stromatic tissues** occasionally intermingled with host tissue, at base and side pseudoparenchymatous, *textura angularis*, mostly consisting of a few layers of compressed cells, pale brown, 3–11 ( $6.2 \pm 1.90 \mu\text{m}$ ,  $n=50$ ) thick, infrequently outermost layers consisting of thick-walled cells similar to neck tissues 20–45 ( $28.7 \pm 7.04 \mu\text{m}$ ,  $n=16$ ) thick; around neck pseudoparenchymatous, *textura globulosa*, composed of thick-walled, olivaceous black cells, 13–61 ( $35.3 \pm 10.8 \mu\text{m}$ ,  $n=35$ ) thick. **Conidiophores** hyaline, formed along inner locular wall, branched at base, along the length immediately below transverse septa, smooth, septate, cylindrical, straight or irregular. **Paraphyses** present but scarce. **Conidiogenous cells** hyaline, phialidic, integrated, determinate, forming conidia from apical or lateral apertures immediately below transverse septa, subulate, lageniform to cylindrical,  $4\text{--}12 \times 1\text{--}2$  ( $7.2 \pm 1.49 \times 1.6 \pm 0.2 \mu\text{m}$ ,  $n=50$ ). **Conidia** hyaline, cylindrical, aseptate, pointed towards base, oozing in slimy yellow masses,  $2\text{--}4 \times 1$  ( $3.2 \pm 0.26 \times 1.1 \pm 0.08$ ,  $n=50$ )  $\mu\text{m}$ .

**Culture characteristics:** On 2% MEA in the dark at 25°C after 28 days showing circular growth with uneven edges, mycelium flat to fluffy, above white with randomly distributed small patches of luteous shade, cottony clumps formed near the edges, orange granular-like conidiomata present when fertile; at 30°C mycelium fluffy to cottony, white above with large patches of luteous shade, often concentrated in centre. Optimum growth at 25°C with growth rate of 5.1 mm/day, followed by 30°C (4.0 mm/day), 20°C (3.1 mm/day), 15°C (1.8 mm/day), 10°C (0.9 mm/day), 35°C (0.4 mm/day), and 5°C (0.4 mm/day).

**Host:** *Eucalyptus urophylla*  $\times$  *E. grandis*, *E. grandis*, *Corymbia henryi*.

**Distribution:** South Africa (KwaZulu-Natal).

**Additional materials examined:** South Africa, KwaZulu-Natal, Mtubatuba. Bark of *Eucalyptus urophylla*  $\times$  *E. grandis*. January 2021. J. Roux. (PRU(M) 4505, CMW 57827, CMW-IA 164). GenBank: PP058402 (ITS); PP061202 ( $\beta$ -tubulin); PP058421 (LSU); KwaZulu-Natal, KwaNgwanase. Bark of *Corymbia henryi*. 21 October 2020. H. Suzuki & M. J. Wingfield. (PRU(M) 4506; culture CMW 56597, CMW-IA 165). GenBank: PP058388 (ITS); PP061188 ( $\beta$ -tubulin); PP058407 (LSU); (PRU(M) 4507; culture CMW 56611, CMW-IA 166). GenBank: PP058392 (ITS); PP061192 ( $\beta$ -tubulin); PP058411 (LSU).

**Notes:** *Xanthoportha* shows a close affinity to *Parvomorbus* in multigene phylogenetic analyses, and the two genera are clustered close to seven other genera in the Family, including *Aurapex*, *Corticomorbus*, *Cryptonectria*, *Cryptometrion*, *Diversimorbus*, *Holocryphia* and *Luteocirrhus*. Morphologically, *Xanthoportha* differs from *Cryptonectria*, *Corticomorbus*, *Cryptometrion* and *Diversimorbus* in having aseptate ascospores, whereas the others have 1-septate ascospores (Chen et al., 2016; Chen, Wingfield, & Roux, 2013; Gryzenhout et al., 2009, 2010). *Holocryphia* spp. produce aseptate ascospores similar to *X. myrticola* but differ in ascospore shape and dimensions. *Holocryphia* spp. produce cylindrical to fusiform ascospores, while *X. myrticola* (ascospores:  $7\text{--}12 \times 2\text{--}3.5 \mu\text{m}$ ) produces fusoid to oval shape ascospores, which are wider than those of *Holocryphia* spp.:

*H. capensis* ( $5\text{--}12 \times 1.2\text{--}2 \mu\text{m}$ ), *H. eucalypti* ( $4.5\text{--}12.5 \times 0.5\text{--}2 \mu\text{m}$ ), *H. gleniana* ( $6.5\text{--}14 \times 1.2\text{--}2.3 \mu\text{m}$ ) and *H. mzansi* ( $8\text{--}16 \times 1.4\text{--}2.4 \mu\text{m}$ ) (Chen, Wingfield, & Roux, 2013; Gryzenhout et al., 2006).

Among the nine closely clustered genera, *Aurapex*, *Luteocirrhus* and *Parvomorbus* are known only based on an asexual state (Crane & Burgess, 2013; Gryzenhout et al., 2006; Wang et al., 2020). Morphologically, *Xanthoportha* differs from *Aurapex* in having conical to sub-globose conidiomata with short, stout necks, compared to *Aurapex* which has long, cylindrical to attenuated orange necks (Gryzenhout et al., 2006), and from *Luteocirrhus* in having periphysate ostiolar necks which are absent in *L. shearii* (Crane & Burgess, 2013).

*Parvomorbus* shows the closest affinity to *Xanthoportha* as a sister clade. It is a recently established genus, accommodating two species, *Parvomorbus eucalypti* and *P. guangdongensis*, isolated from *Eucalyptus* hybrids in China (Wang et al., 2020). Their conidiomata are slightly immersed or superficial in the substrate, whereas the conidiomata of *X. myrticola* are deeply immersed in the substrate with a stout neck protruding just above the substrate. Wang et al. (2020) described the conidiomata of *Parvomorbus* spp. as having no necks. Conidiomatal necks of *X. myrticola* are short, stout and not attenuated, which are well-defined by the presence of paraphyses and a well-developed stromatal structure around the necks. Apart from conidiomatal morphology, they also show different growth preferences. *X. myrticola* grows at 5°C, and optimum growth occurs at 25°C, whereas *Parvomorbus* spp. do not grow at 5°C and their optimal growth temperature is 30°C.

### 3.4 | Pathogenicity tests

Six weeks after inoculation, the two isolates produced lesions on the three *E. grandis* varieties (TAG5, GC540, ZG14) and *C. henryi* (Figures 5 and 6). Statistical analyses showed that lesion lengths were significantly different between the inoculated plants and the controls. They were also significantly different between the *E. grandis* varieties, with those on the pure *E. grandis* varieties (TAG5, ZG14) being larger ( $19.2 \pm 5.2$  mm [mean  $\pm$  SD] and  $19.1 \pm 3.4$  mm, respectively), than on the hybrid *E. grandis*  $\times$  *E. camaldulensis* (GC 540) variety ( $12.2 \pm 3.8$  mm; Figure 7). The lesion lengths on the *C. henryi* saplings were an average of  $45.3 \pm 30.6$  mm. Wounds made for control inoculations were covered with callus, and stem discolouration was equal in length to the size of the original inoculation wound. Reisolations from the diseased plants, but not the controls, gave rise to the inoculated fungus, the identity of which was confirmed based on culture characteristics.

## 4 | DISCUSSION

This study resulted in the discovery of a new fungal canker pathogen of *Eucalyptus* and *Corymbia* in South Africa. The fungus resides in the Cryphonectriaceae, well known to accommodate numerous species that cause canker diseases on these trees. Morphological features

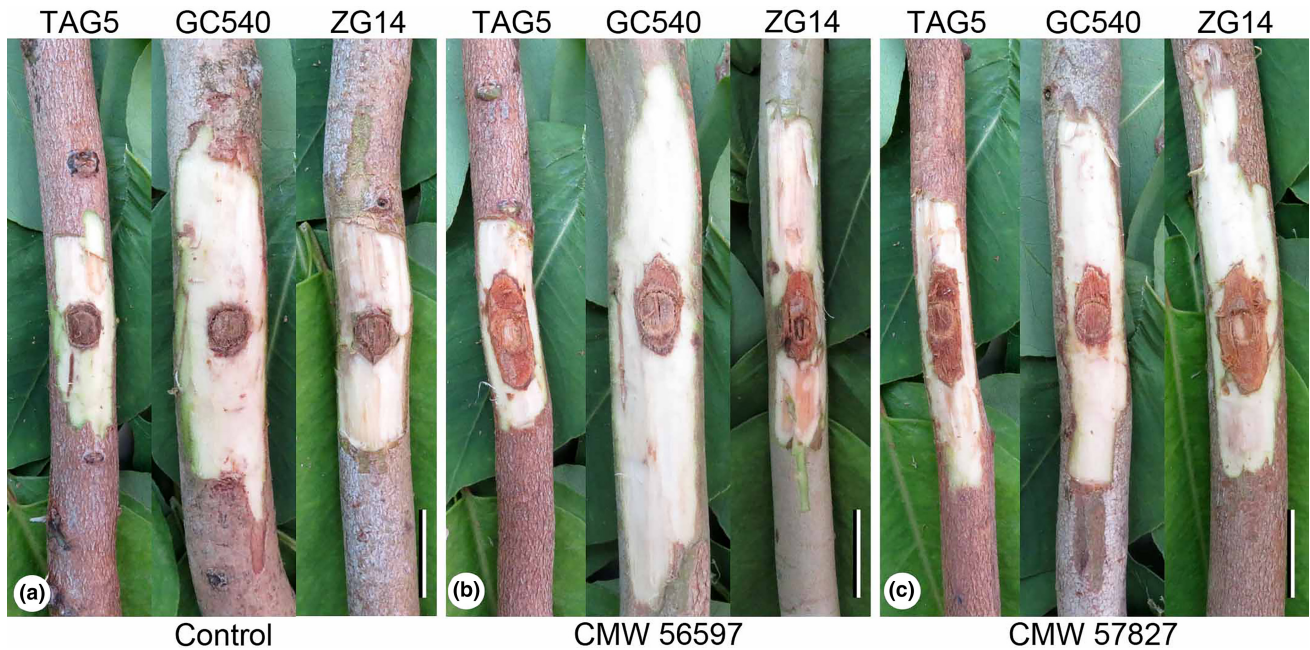


**FIGURE 5** Pathogenicity tests on *Eucalyptus grandis* varieties (TAG5, GC540, ZG14, left to right in each image) inoculated with agar discs as a control (a), or with discs taken from the actively growing edges of 14-day-old cultures of isolates CMW 56597 (b) and CMW 57827 (c). Scale bars: a–c = 10 mm.

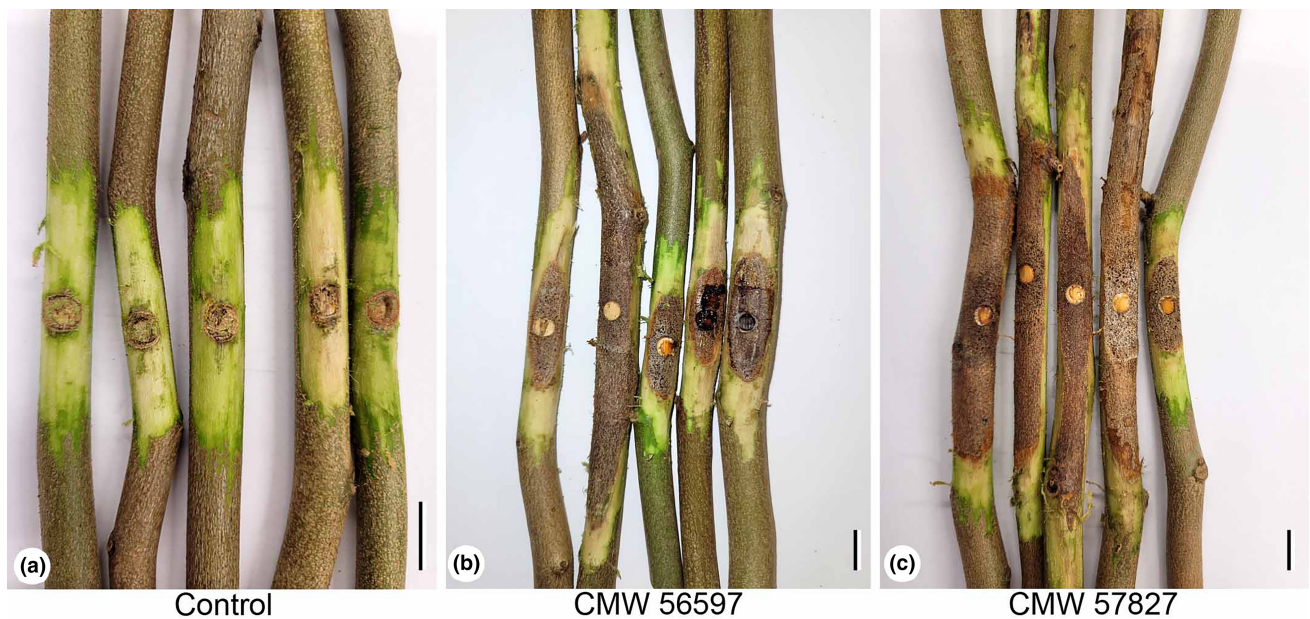


**FIGURE 6** Pathogenicity tests on stems of *Corymbia henryi* saplings inoculated with agar discs as a control (a) or with discs taken from the actively growing edges of 14-day-old cultures of isolates CMW 56597 (b) and CMW 57827 (c). Scale bars: a–c = 10 mm.

of the fungus and phylogenetic analyses based on DNA sequence data led to the conclusion that the fungus is best accommodated in a novel genus and species, for which the name *X. myrticola* is provided. Pathogenicity tests on *Eucalyptus* varieties and *C. henryi* saplings showed that *X. myrticola* was able to cause disease.

*X. myrticola* is phylogenetically closely related to species in the genus *Parvomorbus*, which are known to infect *Eucalyptus* trees in

China (Wang et al., 2020). Our decision to place the fungus in a discrete genus was guided by differences in morphological features that have been used to distinguish genera in the Cryphonectriaceae and that are distinct from *Parvomorbus*. Importantly, this decision was strengthened by the fact that species of *Parvomorbus* are known only in China, and we would not wish to imply a connection to a disease in that country. We do, however, recognize that

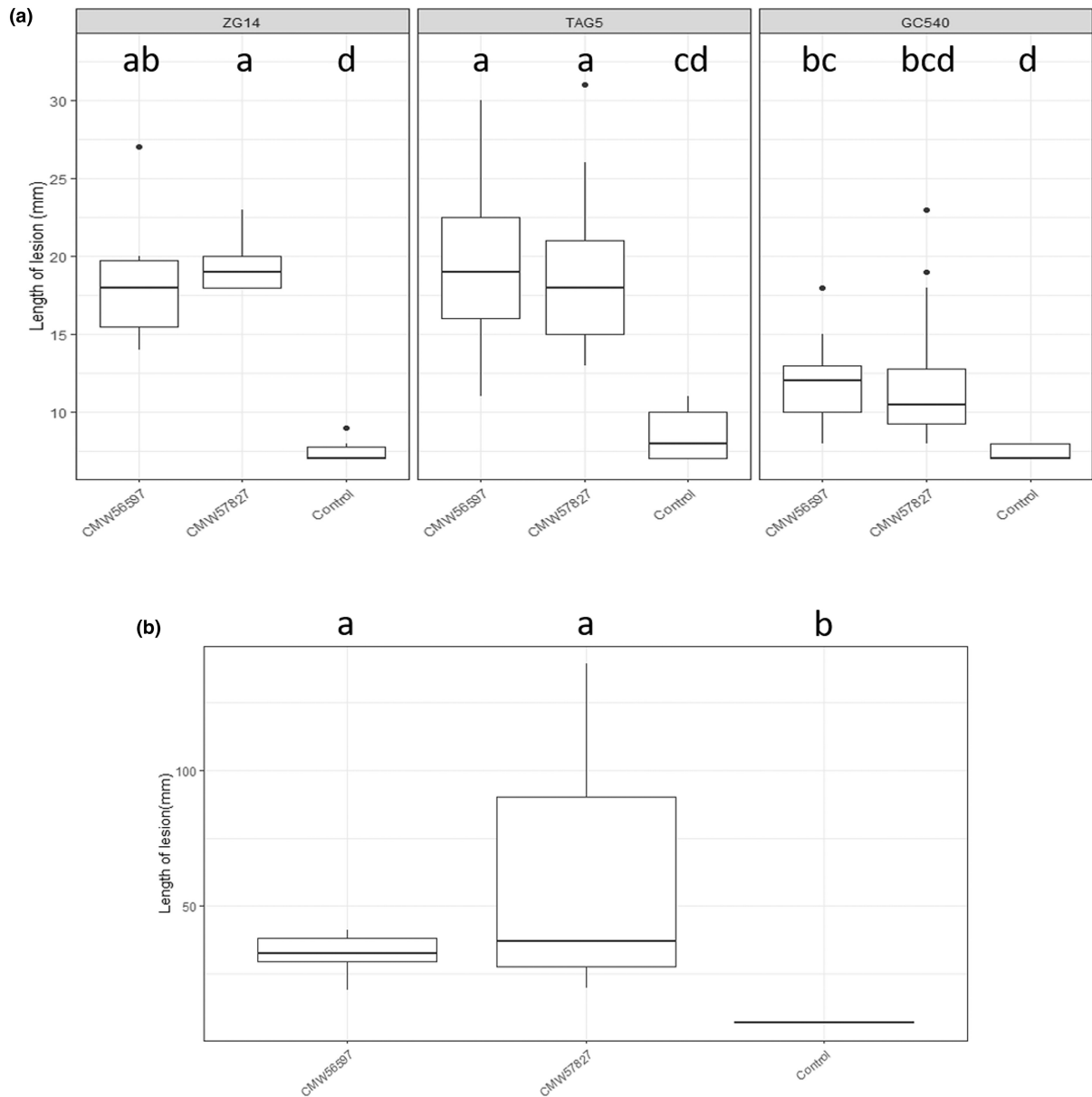


**FIGURE 7** Boxplots of lesion lengths resulting from pathogenicity trials on *Eucalyptus grandis* varieties TAG5, GC540, and ZG14 (a) and on *Corymbia henryi* (b) inoculated with isolates CMW 56597 and CMW 57827 or agar disc as a control. Different letters indicate significant differences in pathogenicity based on the Games–Howell post hoc test in (a) and Steel–Dwass test in 7(b) ( $p < 0.05$ ).

genera are taxonomic units of convenience and that a future revision of the genera in the Cryphonectriaceae may lead to a different decision.

The fact that the disease caused by *X. myrtilcola* occurs on both *Eucalyptus* and *Corymbia* is relevant. *Eucalyptus* and *Corymbia* are closely related but also distinct, and this is also true for many of the insect pests and pathogens that infect them. For example, the aggressive leaf and shoot pathogen *Teratosphaeria destructans* (Aylward et al., 2019; Wingfield et al., 1996) infects many species of *Eucalyptus* and never those of *Corymbia*. Similarly, species of *Quambalaria* differentiate between these hosts, with *Quambalaria pitireka* infecting *Corymbia* spp. and *Q. eucalypti* specific to *Eucalyptus* (Pegg et al., 2008). In the case of the

Cryphonectriaceae, however, the *Eucalyptus* canker pathogen *C. austroafricana* has recently been found for the first time on *Corymbia* (Suzuki et al., 2023). This supports the view that many species of the Cryphonectriaceae have relatively wide host ranges that extend beyond genera, yet within the confines of host ordinal boundaries.

The origin of *X. myrtilcola* is unknown, but the disease appears to have emerged relatively recently. We base this view on the fact that disease surveys are regularly conducted in South African eucalypt plantations, and it seems unlikely that it would have gone unnoticed for a long period of time. In the area where the disease became obvious, only a single hybrid variety of *E. urophylla* × *E. grandis* was infected. This is not uncommon for *Eucalyptus* pathogens that are

typically very specific to single genotypes of these host trees (Van Heerden et al., 2005; Wingfield et al., 2013). In the case of *Corymbia*, species in this genus are relatively new to the South African plantation environment, and the disease caused by *X. myrticola* would likewise be new to these trees. A host shift (Slippers et al., 2005) from a native species in the Myrtales to infect the trees reported in this study is a distinct possibility, given the fact that this has occurred for other species in the Cryphonectriaceae (Nakabonge, Roux, et al., 2006; Oliveira et al., 2022; Suzuki et al., 2022).

The relative importance of *X. myrticola* and the disease that it causes has yet to be determined. The fungus has so far been found only in the KwaZulu-Natal region of South Africa and at a relatively limited level. Its known occurrence is restricted to an area that has a subtropical climate, suggesting it is best suited to that environment. This represents a relatively small portion of the *Eucalyptus*-growing area of South Africa. A similar situation is true for *C. austroafricana*, which also only occurs on *Eucalyptus* in the subtropical areas of the country and has been managed through an active programme of breeding and selection (Nakabonge, Roux, et al., 2006; Van Heerden et al., 2005). Future surveys and disease monitoring activities are required to determine the distribution of *X. myrticola* and the relative threat it poses to plantation forestry in South Africa.

## ACKNOWLEDGEMENTS

We thank Mxolisi Silinda, who first recognized the disease on *C. henryi* and reported this to us. We are grateful for financial support for this study provided by members of the Tree Protection Co-operative Programme (TPCP) South Africa and a postdoctoral fellowship provided to the first author by the University of Pretoria.

## DATA AVAILABILITY STATEMENT

The datasets generated and/or analyses carried out during the current study are available from the corresponding author upon reasonable request.

## ORCID

Hiroyuki Suzuki  <https://orcid.org/0000-0002-9301-9207>

## REFERENCES

- Ali, D.B., Marincowitz, S., Wingfield, M.J., Roux, J., Crous, P.W. & McTaggart, A.R. (2018) Novel Cryphonectriaceae from La Réunion and South Africa, and their pathogenicity on *Eucalyptus*. *Mycological Progress*, 17, 953–966.
- Anagnostakis, S.L. & Kranz, J. (1987) Population dynamics of *Cryphonectria parasitica* in a mixed-hardwood forest in Connecticut. *Phytopathology*, 77, 751–754.
- Aylward, J., Roets, F., Dreyer, L.L. & Wingfield, M.J. (2019) *Teratosphaeria* stem canker of *Eucalyptus*: two pathogens, one devastating disease. *Molecular Plant Pathology*, 20, 8–19.
- Begoude, A.D., Gryzenhout, M., Wingfield, M.J. & Roux, J. (2010) *Aurifilum*, a new fungal genus in the Cryphonectriaceae from *Terminalia* species in Cameroon. *Antonie Van Leeuwenhoek*, 98, 263–278.
- Beier, G.L., Hokanson, S.C., Bates, S.T. & Blanchette, R.A. (2015) *Aurantioportha corni* gen. et comb. nov., an endophyte and pathogen of *Cornus alternifolia*. *Mycologia*, 107, 66–79.
- Chen, S., Liu, Q.L., Li, G.Q., Wingfield, M.J. & Roux, J. (2018) A new genus of Cryphonectriaceae isolated from *Lagerstroemia speciosa* in southern China. *Plant Pathology*, 67, 107–123.
- Chen, S., Wingfield, M.J., Li, G.Q. & Liu, F.F. (2016) *Corticimorbus sinomyrti* gen. et sp. nov. (Cryphonectriaceae) pathogenic to native *Rhodomyrtus tomentosa* (Myrtaceae) in South China. *Plant Pathology*, 65, 1254–1266.
- Chen, S., Wingfield, M.J., Roets, F. & Roux, J. (2013) A serious canker disease caused by *Immersiporthe knoxdaviesiana* gen. et sp. nov. (Cryphonectriaceae) on native *Rapanea melanophloeos* in South Africa. *Plant Pathology*, 62, 667–678.
- Chen, S., Wingfield, M.J. & Roux, J. (2013) *Diversimorbus metrosiderotis* gen. et sp. nov. and three new species of *Holocryphia* (Cryphonectriaceae) associated with cankers on native *Metrosideros angustifolia* trees in South Africa. *Fungal Biology*, 117, 289–310.
- Crane, C. & Burgess, T.I. (2013) *Luteocirrhus shearii* gen. sp. nov. (Diaporthales, Cryphonectriaceae) pathogenic to Proteaceae in the South Western Australian floristic region. *IMA Fungus*, 4, 111–122.
- Ferreira, M.A., Oliveira, M.E.S., Silva, G.A., Mathioni, S.M. & Mafia, R.G. (2019) *Capillaureum caryovora* gen. sp. nov. (Cryphonectriaceae) pathogenic to pequi (*Caryocar brasiliense*) in Brazil. *Mycological Progress*, 18, 385–403.
- Glass, N.L. & Donaldson, G.C. (1995) Development of primer sets designed for use with the PCR to amplify conserved genes from filamentous ascomycetes. *Applied and Environmental Microbiology*, 61, 1323–1330.
- Gryzenhout, M., Myburg, H., Rodas, C.A., Wingfield, B.D. & Wingfield, M.J. (2006) *Aurapex penicillata* gen. sp. nov. from native *Miconia theaezans* and *Tibouchina* spp. in Colombia. *Mycologia*, 98, 105–115.
- Gryzenhout, M., Myburg, H., Van der Merwe, N.A., Wingfield, B.D. & Wingfield, M.J. (2004) *Chrysoportha*, a new genus to accommodate *Cryphonectria cubensis*. *Studies in Mycology*, 50, 119–142.
- Gryzenhout, M., Tarigan, M., Clegg, P.A. & Wingfield, M.J. (2010) *Cryptometrion aestuescens* gen. sp. nov. (Cryphonectriaceae) pathogenic to *Eucalyptus* in Indonesia. *Australasian Plant Pathology*, 39, 161–169.
- Gryzenhout, M., Wingfield, B.D. & Wingfield, M.J. (2009) *Taxonomy, phylogeny, and ecology of bark-inhabiting and tree-pathogenic fungi in the Cryphonectriaceae*. St Paul, MN: American Phytopathological Society.
- Guindon, S., Dufayard, J.F., Lefort, V., Anisimova, M., Hordijk, W. & Gascuel, O. (2010) New algorithms and methods to estimate maximum likelihood phylogenies: assessing the performance of PhyML 3.0. *Systematic Biology*, 59, 307–321.
- Huang, H.Y., Huang, H.H., Zhao, D.Y., Shan, T.J. & Hu, L.L. (2022) *Pseudocryphonectria elaeocarpicola* gen. et sp. nov. (Cryphonectriaceae, Diaporthales) causing stem blight of *Elaeocarpus* spp. in China. *MycKeys*, 91, 67–84.
- Jiang, N., Fan, X., Tian, C. & Crous, P.W. (2020) Reevaluating Cryphonectriaceae and allied families in Diaporthales. *Mycologia*, 112, 267–292.
- Katoh, K., Rozewicki, J. & Yamada, K.D. (2019) MAFFT online service: multiple sequence alignment, interactive sequence choice and visualisation. *Briefings in Bioinformatics*, 20, 1160–1166.
- Kumar, S., Stecher, G. & Tamura, K. (2016) MEGA7: molecular evolutionary genetics analysis version 7.0 for bigger datasets. *Molecular Biology and Evolution*, 33, 1870–1874.
- Nakabonge, G., Gryzenhout, M., Roux, J., Wingfield, B.D. & Wingfield, M.J. (2006) *Celoportha dispersa* gen. et sp. nov. from native Myrtales in South Africa. *Studies in Mycology*, 55, 255–267.
- Nakabonge, G., Roux, J., Gryzenhout, M. & Wingfield, M.J. (2006) Distribution of *Chrysoportha* canker pathogens on *Eucalyptus* and *Syzygium* spp. in eastern and southern Africa. *Plant Disease*, 90, 734–740.

- Oliveira, M.E.S., Kanzi, A.M., Van der Merwe, N.A., Wingfield, M.J., Wingfield, B.D., Silva, G.A.S. et al. (2022) Genetic variability in populations of *Chrysosporthe cubensis* from Brazil. *Australasian Plant Pathology*, 51, 175–191.
- Pegg, G.S., O'Dwyer, C., Carnegie, A.J., Burgess, T.I., Wingfield, M.J. & Drenth, A. (2008) *Quambalaria* species associated with plantation and native eucalypts in Australia. *Plant Pathology*, 57, 702–714.
- Pohlert, T. (2020) *PMCMRplus: calculate pairwise multiple comparisons of mean rank sums extended*. R package version 1.4.4. Available from: <https://cran.r-project.org/web/packages/PMCMRplus/PMCMRplus.pdf> [Accessed 7th February 2024].
- Posada, D. (2008) jModelTest: phylogenetic model averaging. *Molecular Biology and Evolution*, 25, 1253–1256.
- R Core Team. (2019) *R: a language and environment for statistical computing*. Vienna, Austria: R Foundation for Statistical Computing. Available from: <http://www.R-project.org/> [Accessed 7th February 2024].
- Rauf, M.R.B.A., McTaggart, A.R., Marincowitz, S., Barnes, I., Japarudin, Y. & Wingfield, M.J. (2019) Pathogenicity of *Chrysosporthe deuterocubensis* and *Myrtoporthe bodenii* gen. et sp. nov. on *Eucalyptus* in Sabah, Malaysia. *Australasian Plant Pathology*, 49, 53–64.
- Rehner, S.A. & Samuels, G.J. (1994) Taxonomy and phylogeny of *Gliocladium* analysed from nuclear large subunit ribosomal DNA sequences. *Mycological Research*, 98, 625–634.
- Ronquist, F., Teslenko, M., Van der Mark, P., Ayres, D.L., Darling, A., Höhna, S. et al. (2012) MrBayes 3.2: efficient Bayesian phylogenetic inference and model choice across a large model space. *Systematic Biology*, 61, 539–542.
- Shiffler, R.E. (1988) Maximum Z scores and outlier. *The American Statistician*, 42, 79–80.
- Slippers, B., Stenlid, J. & Wingfield, M.J. (2005) Emerging pathogens: fungal host jumps following anthropogenic introduction. *Trends in Ecology & Evolution*, 20, 420–421.
- Suzuki, H., Marincowitz, S., Roux, J., Wingfield, B.D. & Wingfield, M.J. (2023) First report of canker caused by *Chrysosporthe austroafricana* on the plantation-grown eucalypt *Corymbia henryi* in South Africa. *Forestry*, 96, 509–517.
- Suzuki, H., Marincowitz, S., Wingfield, B.D. & Wingfield, M.J. (2022) Genetic diversity and population structure of *Chrysosporthe deuterocubensis* isolates from *Melastoma* and *Eucalyptus* in Malaysia and Indonesia. *Forest Pathology*, 52, e12762.
- Van Heerden, S.W., Amerson, H.V., Preisig, O., Wingfield, B.D. & Wingfield, M.J. (2005) Relative pathogenicity of *Cryphonectria cubensis* on *Eucalyptus* clones differing in their resistance to *C. cubensis*. *Plant Disease*, 89, 659–662.
- Vermeulen, M., Gryzenhout, M., Wingfield, M.J. & Roux, J. (2011) New records of the Cryphonectriaceae from southern Africa including *Latruncellus aurorae* gen. sp. nov. *Mycologia*, 103, 554–569.
- Vermeulen, M., Gryzenhout, M., Wingfield, M.J., Roux, J. & Holdenrieder, O. (2013) Population structure of *Chrysosporthe austroafricana* in Southern Africa determined using vegetative compatibility groups (VCGs). *Forest Pathology*, 43, 124–131.
- Vilgalys, R. & Hester, M. (1990) Rapid genetic identification and mapping of enzymatically amplified ribosomal DNA from several *Cryptococcus* species. *Journal of Bacteriology*, 172, 4238–4246.
- Wang, W., Li, G.Q., Liu, Q.L. & Chen, S.F. (2020) Cryphonectriaceae on Myrtales in China: phylogeny, host range, and pathogenicity. *Persoonia*, 45, 101–131.
- White, T.J., Bruns, T., Lee, S. & Taylor, J. (1990) Amplification and direct sequencing of fungal ribosomal RNA genes for phylogenetics. In: Innis, M.A., Gelfand, D.H., Sninsky, J.J. & White, T.J. (Eds.) *PCR protocols: a guide to methods and applications*. New York: Academic Press, pp. 315–322.
- Wingfield, M.J. (2003) Increasing threat of diseases to exotic plantation forests in the Southern Hemisphere: Lessons from *Cryphonectria* canker. *Australasian Plant Pathology*, 32, 133–139.
- Wingfield, M.J., Crous, P.W. & Boden, D. (1996) *Kirramyces destructans* sp. nov., a serious leaf pathogen of *Eucalyptus* in Indonesia. *South African Journal of Botany*, 62, 325–327.
- Wingfield, M.J., Roux, J., Slippers, B., Hurley, B.P., Garnas, J., Myburg, A.A. et al. (2013) Established and new technologies reduce increasing pest and pathogen threats to Eucalypt plantations. *Forest Ecology and Management*, 301, 35–42.
- Wingfield, M.J., Swart, W.J. & Aveal, B.J. (1989) First record of *Cryphonectria* canker of *Eucalyptus* in South Africa. *Phytophylactica*, 21, 311–313.

## SUPPORTING INFORMATION

Additional supporting information can be found online in the Supporting Information section at the end of this article.

**How to cite this article:** Suzuki, H., Marincowitz, S., Roux, J., Paap, T., Wingfield, B.D. & Wingfield, M.J. (2024) A new genus and species of Cryphonectriaceae causing stem cankers on plantation eucalypts in South Africa. *Plant Pathology*, 00, 1–14. Available from: <https://doi.org/10.1111/ppa.13883>